Supplementary Materials for

Rapid nitrous oxide cycling in the suboxic ocean

Andrew R. Babbin,* Daniele Bianchi, Amal Jayakumar, Bess B. Ward

*Corresponding author. E-mail: babbin@mit.edu

Published 5 June 2015, *Science* **348**, 1127 (2015)
DOI: 10.1126/science.aaa8380

This PDF file includes:

Other Supplementary Material for this manuscript includes the following:
(available at www.sciencemag.org/cgi/content/full/348/6239/1127/DC1)

1D model code and output as zipped file

Materials and Methods

Sample collection and concentration measurements

Sampling was conducted onboard the R/V *Thomas G. Thompson* cruise TN278 in March and April 2012 in the Eastern Tropical North Pacific (ETNP) oxygen minimum zone (OMZ) off the coast of Mexico. Depth profiles for oxygen, N_2O, and nitrite concentrations were collected by multiple CTD casts (Fig. S1) using a CTD rosette with twenty-four 12 L Niskin bottles. Dissolved oxygen was measured using an in situ Seabird membrane sensor (SBE 43) attached to the CTD package, nitrite using an AutoAnalyzer with standard spectrophotometric techniques (*39*), and N_2O with a gas chromatograph (GC) with an electron capture detector (Shimadzu) (*40*). Samples for N_2O were collected in 160 mL serum bottles by overfilling three times and capping immediately. N_2O was measured immediately by sequential head-space equilibration of equal volumes (25 mL) of seawater sample and helium (*25, 41*). 0.5 mL of each extraction was injected into a Shimadzu gas chromatograph Model GC–8A with an electron capture detector and a 2 m × 2.2 mm inner diameter Haysep D column (80/100 mesh). The column temperature was set to 30 °C, while the injection port and detector were maintained at 50 and 300 °C, respectively. Analyses were standardized using ambient air and a 1 ppm N_2O standard (Scott Gas).

N_2O reduction rate incubations

At three stations, N_2O reduction rates were directly measured at 8 depths within the oxycline and the core of the anoxic water, adapting the methods of Bulow et al. (*42*). The three sites consisted of a coastal site “Station 1” (20.1 °N 106.0 °W; bottom depth

2200 m) and two offshore sites “Station 2” (16.5 °N 107.2 °W; bottom depth 3600 m) and “Station 3” (16.0 °N 110.0 °W; bottom depth 3300 m). Water for incubations was collected from Niskin bottles by overflowing 300 mL ground glass stoppered bottles three times before being transferred into a N_2 flushed glove bag for aliquoting into incubation vials. 12 mL Exetainers (Labco, UK) with previously degassed septa were filled with 8 mL of seawater for incubation and purged with He for 5 minutes. Doubly-labeled $(^{15}N)_2O$ (Cambridge Isotope) was injected after He-purging using a gas-tight syringe to a final concentration of 30 nmol L^{-1}. We assumed any preexisting N_2O was removed during the He-purging, giving a 100% isotopic label fraction. Triplicate vials were poisoned with 50% (w/v) zinc chloride at 5 time points spanning 36 hr (coastal site) or 48 hr (offshore sites) after incubation at 10 °C in the dark. Accumulation of $^{30}N_2$ was measured on an isotope ratio mass spectrometer (Europa 20/20) with an in-line liquid nitrogen trap to remove excess labeled N_2O.

Estimate of N_2O production rates

A steady state one-dimensional advection-diffusion-reaction balance with depth (z) was developed to calculate the N_2O production rate (P) from the reduction rate (R) measurement and the structure of the N_2O concentration (C) profile:

$$P = R - v\frac{\partial C}{\partial z} - D\frac{\partial^2 C}{\partial z^2} \ .$$

We assumed a constant advection coefficient (v) of 1×10^{-7} m/s, and a constant diffusivity coefficient (D) of 2×10^{-5} m^2/s consistent with previous studies in the ETNP (*19*) as well as analogous regions in the tropics (*43*, *44*). As both the consumption via reduction and concentration profiles were measured, the production rate is the only

calculated variable. This calculation assumes a steady state in the concentration profile and the only biological loss term of N_2O is reduction to N_2. The calculated production rates showed minimal sensitivity to the choice of upwelling, and limited sensitivity to the choice of vertical diffusion for typically observed values, as shown in Fig. S2 (top panel).

The choice of a 1–D approach is dictated here by the limited number of profiles of measured reduction rates, and the limited ability of current 3–D models in capturing the circulation, O_2 distribution and biogeochemistry of OMZ (e.g. (*45*)). A 1–D approach is well-suited to a process-oriented study of the OMZ, which are characterized by weak lateral circulation and large vertical gradients in chemical properties. However, because the results presented here regarding the imbalance of N_2O production and consumption depend on physical transports, we performed an additional suite of sensitivity analyses, including a parameterization of lateral transports through a restoring term (see section **Parameterization of horizontal transport**). This second sensitivity suite of runs shows that imbalances > 1 nmol L^{-1} d^{-1} are readily produced at the top of the OMZ for realistic diffusivities (> 10^{-5} m^2 s^{-1}), upwelling velocities and horizontal restoring timescale (Fig. S2).

Estimation of OMZ size

Gridded oxygen concentrations from the World Ocean Atlas 2009 dataset (*46*) were corrected using the method of Bianchi et al. (*28*). The areal expanse and volume of the ETNP were numerically integrated using the thresholds of 20 µmol L^{-1} O_2 concentration for suboxia and 2.5 µmol L^{-1} for anoxia.

One dimensional biogeochemistry model of the ETNP OMZ

We implemented a mechanistic 1–D model of the biogeochemistry of the ETNP OMZ that describes the cycling of organic matter, here represented by particulate organic carbon (POC), and of dissolved phosphate (PO_4^{3-}), nitrate (NO_3^-), oxygen (O_2), and nitrous oxide (N_2O). While the model includes several tracers for completeness, it is developed to explicitly target the cycling of N_2O along the gradients between oxygenated and anoxic waters. Models of this type have a rich history in ocean biogeochemistry, starting from the early work of Wyrtki (*47*) and Munk (*48*), to include recent efforts devoted to OMZ and N_2O dynamics, such as in Yamagishi et al. (*19*). As in earlier studies, our model solves for the steady state balance between biogeochemical sources and sinks (aerobic respiration, nitrification and denitrification) and physical transport (advection, turbulent diffusion and gravitational sinking) of tracers in the water column. The values of the parameters used are listed in Table S1. The equations are:

$$\frac{\partial(\mathrm{w_{sink}}\cdot \mathrm{POC})}{\partial \mathrm{z}} = -\mathrm{Remin} - \mathrm{Denit}$$

$$\frac{\partial\left(\mathrm{w_{up}}\cdot \mathrm{PO_4^{3-}}\right)}{\partial \mathrm{z}} - \frac{\partial}{\partial \mathrm{z}}\left(\mathrm{D_z}\frac{\partial \mathrm{PO_4^{3-}}}{\partial \mathrm{z}}\right) = \mathrm{r_{P:C}^{rem}Remin} + \mathrm{r_{P:C}^{den}Denit}$$

$$\frac{\partial\left(\mathrm{w_{up}}\cdot \mathrm{NO_3^-}\right)}{\partial \mathrm{z}} - \frac{\partial}{\partial \mathrm{z}}\left(\mathrm{D_z}\frac{\partial \mathrm{NO_3^-}}{\partial \mathrm{z}}\right) = \mathrm{r_{N:C}^{rem}Remin} - \mathrm{r_{N:C}^{den}Denit}$$

$$\frac{\partial\left(\mathrm{w_{up}}\cdot \mathrm{O_2}\right)}{\partial \mathrm{z}} - \frac{\partial}{\partial \mathrm{z}}\left(\mathrm{D_z}\frac{\partial \mathrm{O_2}}{\partial \mathrm{z}}\right) = \mathrm{r_{O_2:C}^{rem}Remin}$$

$$\frac{\partial\left(\mathrm{w_{up}}\cdot \mathrm{N_2O}\right)}{\partial \mathrm{z}} - \frac{\partial}{\partial \mathrm{z}}\left(\mathrm{D_z}\frac{\partial \mathrm{N_2O}}{\partial \mathrm{z}}\right) = \mathrm{S_{N_2O}^{+nit}} + \mathrm{S_{N_2O}^{+den}} - \mathrm{S_{N_2O}^{-den}}$$

In each equation, the left hand side represents the physical transport, and the right-hand side the biogeochemical sources and sinks. Here, w_{sink} is the sinking speed of organic particles, w_{up} is the upwelling velocity and D_z is the vertical turbulent diffusion coefficient, which are in general functions of depth. The *r* terms are stoichiometric ratios. As discussed in the previous sections (see *Estimate of N_2O production rates*), the one-dimensional framework is adequate for representing the processes that take place across the vertical biogeochemical gradients that characterize OMZ. Indeed, because of its formulation (see *Model implementation*), the 1–D model can resolve the fine-scale sharp biogeochemical transitions that characterize the oxycline, which cannot be accurately represented in the current generation of 3–D model owing to their too coarse vertical resolution. For completeness, we tested the effect of including horizontal advection and diffusion terms, as described in the section **Parameterization of horizontal transport**.

The biogeochemical sources and sinks are modeled as described in the following sections.

Remineralization:

$$\mathrm{Remin} = \mathrm{k_{rem}} \cdot \frac{\mathrm{O_2}}{\mathrm{O_2} + \mathrm{K_{O_2}}} \cdot \mathrm{POC}$$

Aerobic remineralization and nitrification processes are modeled as a first order reaction depending on the concentration of POC, and modulated by the dissolved O_2 according to a Michaelis–Menten formulation, in agreement with the oxygen response of nitrifying communities described in Martens-Habbena et al. (*12*).

Denitrification:

$$\mathrm{Denit} = \mathrm{k_{den}} \cdot \frac{\mathrm{NO_3^-}}{\mathrm{NO_3^-} + \mathrm{K_{NO_3^-}}} \cdot \mathrm{e}^{-\frac{\mathrm{O_2}}{\mathrm{K_{O_2}^{den}}}} \cdot \mathrm{POC}$$

The denitrification term describes the set of anaerobic reactions that reduce NO_3^- to N_2O and N_2. We assume that denitrification is an overall heterotrophic process fueled by organic matter, hence the first order dependence on POC. Two limitation factors are introduced: a Michaelis–Menten dependence on dissolved NO_3^-, and an exponential inhibition by dissolved oxygen, in agreement with the results of Dalsgaard et al. (*26*).

N_2O production by nitrification:

$$\mathrm{S_{N_2O}^{+nit}} = \mathrm{H}\left(\mathrm{O_2} - \mathrm{K_{O_2}^{Nev}}\right) \cdot \left(\frac{\mathrm{a_1}}{\mathrm{O_2}} + \mathrm{b_1}\right) \cdot \mathrm{r_{N:C}^{rem}} \cdot \mathrm{Remin}$$

The production of N_2O by nitrification is modeled as described in Nevison et al. (*21*) and in agreement with the experimental data of Goreau et al. (*8*) Following Nevison et al. (*21*), the production of N_2O by nitrification is set to zero below an oxygen threshold $O_2 = K_{O_2}^{Nev}$, using an oxygen-dependent Heaviside step function H.

N_2O production by denitrification:

$$\mathrm{S_{N_2O}^{+den}} = \frac{1}{2} \cdot \mathrm{r_{N:C}^{den}} \cdot \mathrm{Denit}$$

Here we assume that N_2O is an obligate intermediate of denitrification that can escape to the water column, where it can be taken up again and reduced to N_2 by denitrifiers, as described by the next term. This parameterization is only incorporated into the second version of the model.

N_2O consumption by denitrification:

$$S_{N_2O}^{-den} = k_{N_2O} \cdot N_2O \cdot e^{-\frac{O_2}{K_{O_2}^{sink}}}$$

The reduction of N_2O to N_2 during the final step of denitrification follows the simple approach described in Yamagishi et al. (*19*), and we model N_2O reduction as a first order reaction, equivalent to assuming that organic matter is not a limiting substrate. In addition, we introduce an exponential oxygen-dependent inhibition factor after Dalsgaard et al. (*26*) to represent oxygen poisoning of denitrification.

Anaerobic respiration processes other than denitrification (e.g. sulfate reduction) are not explicitly represented in the model. However, NO_3^- is never consumed to completion in the experiments described, in agreement with observations. Furthermore, we do not explicitly model the cycling of NH_4^+ and NO_2^- (including anammox), and we assume that the cycling of these tracers is rapid, and their reservoirs small compared to NO_3^-.

Model implementation

Rather than simulating primary production in the upper layers, we impose a constant flux of organic particles ($\Phi_{POC} = w_{sink}POC$) as the upper boundary condition for POC (*13*). We impose Dirichlet boundary conditions (fixed concentrations) at the top and bottom of the water column for the remaining dissolved tracers, using values from literature (*49*). We assume constant sinking and upwelling velocities w_{sink} and w_{up}, and a depth-dependent vertical diffusion profile D_z that includes a high-diffusion mixed layer that quickly transitions to a low-diffusion water column interior. The model equations are reduced to a first-order nonlinear system by recasting them in terms of the first

derivatives of each variable. The system is solved by a finite difference algorithm using the three-stage Lobatto IIIa formula, as implemented in the MATLAB function *bvp4c*. This formulation allows for an increased vertical resolution in regions of sharp variation, and produces continuous differentiable solutions. For example, considering the conservation equation for O_2, an auxiliary equation is introduced for the first derivative in the vertical direction, and the equation is split into a system of two equations:

$$y_1 = O_2$$

$$y_2 = \frac{\partial O_2}{\partial z}$$

In this way that the conservation equations can be written as a first-order non-linear system:

$$\frac{\partial y_1}{\partial z} = y_2$$

$$\frac{\partial y_2}{\partial z} = \frac{1}{D_z}\left[\left(w_{up} - \frac{\partial D_z}{\partial z}\right) \cdot y_2 + \frac{\partial w_{up}}{\partial z} \cdot y_1 - SMS(y_1)\right]$$

To prevent non-physical negative solutions, the absolute value of each variable is used in the numerical implementation the model.

Model parameters and boundary condition values

We chose the model parameters from the existing literature, or estimated by applying physical and biogeochemical scaling arguments. As with many biogeochemical models, some tuning was required for the parameters not drawn from literature, and we used the observed tracer profiles as our tuning target. A list of the parameter values and the corresponding references is provided in Table S1.

Model sensitivity analysis

To estimate the errors associated with this one-dimensional representation of the biogeochemistry of the OMZ, we ran a full set of Monte Carlo simulations (N = 5000) perturbing each parameter (Table S1) simultaneously. The new parameters are chosen randomly from a Gaussian or gamma (chosen when the parameters cannot be negative) distribution, with the same mean of the baseline run and a standard deviation equal to 25% of the parameter value. The 25% uncertainty is arbitrarily selected, but we chose such a large value to conservatively account for the range of variability. The output was aligned at the depth of the N_2O concentration peak in order to avoid over-smoothing of features that occurs when maxima are spatially separated.

We further sought to assess the 1–D simplification ignoring horizontal terms in modeling the OMZ by including an additional N_2O restoration parameter to represent horizontal advection and diffusion. The term is implemented as a restoration to a "far-field" N_2O concentration (a typical mean profile outside the OMZ, with a subsurface peak ~50 nmol L^{-1} at ~500 m depth (*50*). The timescale for this restoring function was estimate with scaling arguments for typical horizontal advection and turbulent diffusion terms (described in section **Parameterization of horizontal transport**), and is 1.2 yr in the baseline run. The effect of this restoration is a sink of N_2O around the peak, and a source at depth.

A third run that looks solely at the uncertainties of the biogeochemical N_2O production terms $K_{O_2}, K_{O_2}^{Nev}, a_1, b_1, k_{N_2O}^{fast}, K_{O_2}^{den}, K_{O_2}^{sink}$ to separate biological production from physical redistribution of N_2O. The results of these three runs in affecting the N_2O concentration and production profiles are summarized in Table S2. These runs

consistently indicate a deeper net N_2O production rate maximum than concentration maximum, with an oxygen concentration at the N_2O concentration peak ~3–10 µmol L^{-1}, but 1.5 µmol L^{-1} at the net production rate maximum.

Parameterization of horizontal transport

Because the one-dimensional framework does not include explicit horizontal / isopycnal advection and diffusion, we included a parameterization of these horizontal terms based on physical scaling arguments. Assuming the N_2O concentration has a subsurface peak within the OMZ that is affected by a far-field N_2O distribution outside the OMZ (N_2O^{out}) by horizontal advection through the peak and outward diffusion, the horizontal terms in the N_2O conservation equation can be approximated by:

$$-\nabla \cdot (\vec{u} N_2O) \approx \frac{U}{\Delta x}\left(\mathrm{N_2O^{out}} - \mathrm{N_2O}\right) \text{ (advection)}$$
$$\nabla \cdot K_h \nabla \mathrm{N_2O} \approx \frac{2K_h}{\Delta x^2}\left(\mathrm{N_2O^{out}} - \mathrm{N_2O}\right) \text{ (diffusion)}$$

Here U is the scale for horizontal advection into the OMZ (0.01 m/s), Δx the horizontal distance for typical horizontal gradients around the N_2O peak (500 km), K_h a typical eddy horizontal diffusion (1000 m^2/s). The constant 2 in the diffusive term is a geometric factor that arises from assuming diffusion outwards of the N_2O peak in the *x* direction, and homogeneity in the *y* direction. This geometric factor could be different for different geometric assumptions and remains irrelevant the purpose of the scaling.

Combination of the advective and diffusive terms produces a typical restoring timescale for the N_2O profile given by:

$$\tau = \left(\frac{U}{\Delta x} + \frac{2K_h}{\Delta x^2}\right)^{-1}$$

By using the typical values above, the timescale τ becomes ~1.1 yr, and appears to be dominated by advective terms (timescale of ~1.6 yr) rather than diffusive (timescale ~4 yr). Note that the scale of *U* chosen is probably large for the OMZ, and Δx relatively small, meaning that τ is likely a conservative low estimate, and restoring timescales of several years could be possible.

Following this analysis, we tested the influence of the horizontal restoring term of the form:

$$restoring \approx \tau^{-1}\left(N_2O^{out} - N_2O\right)$$

in both the N_2O production estimate from observations (see *Estimate of N_2O production rates*) and the 1D biogeochemical model (see **One dimensional biogeochemistry model of the ETNP OMZ**).

We found that in both cases the impact on the net production rates is minimal (Fig. S3). While smaller than the vertical terms, the horizontal terms provide an additional N_2O sink around the peak so that, to maintain the observed N_2O concentration magnitude, these terms must be balanced by an increased net (biological) source. Thus, excluding the horizontal terms provides a lower estimate of the cycling rates around the N_2O peak.

Lastly, a full sensitivity analysis of the three physical representations included in the model – vertical diffusion, upwelling, and horizontal restoration – was performed by varying the vertical advection velocity, diffusion coefficient, and horizontal restoring timescale (Table S2, Fig. S2). Station 3 is displayed, but all three stations show the same trends. These figures show the magnitude of the maximum imbalance in N_2O production at the top of the OMZ. By this analysis, (1) vertical diffusion should dominate both other

terms, and has to be very low to reduce the imbalance to less than 1 nmol L^{-1} d^{-1}, and (2) the horizontal terms are negligible unless restoring scales are reduced to < 1 yr, at which point this acts as a net sink of N_2O and requires an increase of the net imbalance rate to reproduce concentration observations.

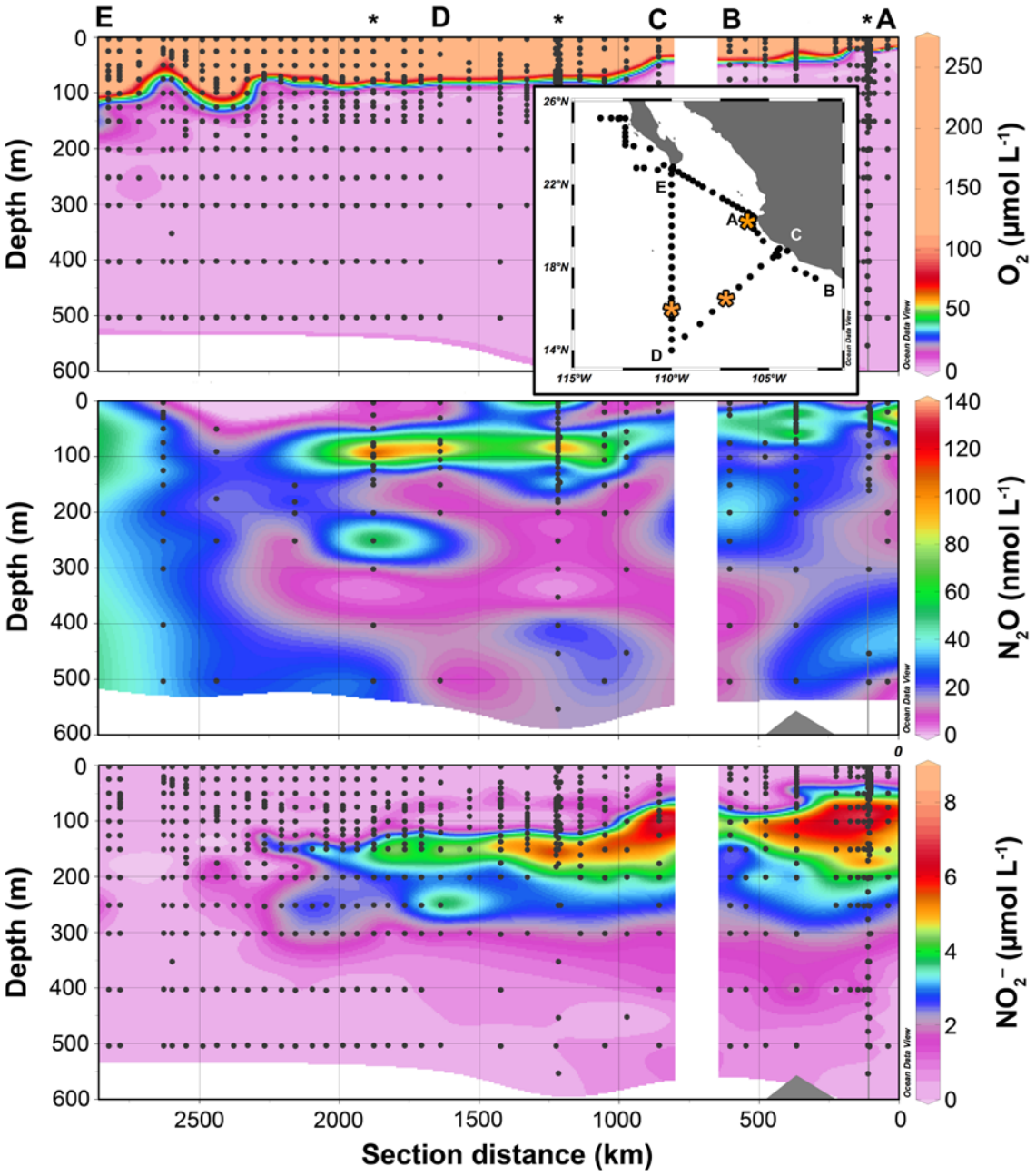

Fig. S1. ETNP biogeochemistry.

Biogeochemical section for (top) oxygen, (middle) N_2O, and (bottom) NO_2^- concentrations. Inset shows map of stations along with waypoints A–E corresponding to sections as shown. Filled points denote concentration sampling sites and orange asterisks indicate the 3 stations at which rate experiments were conducted.

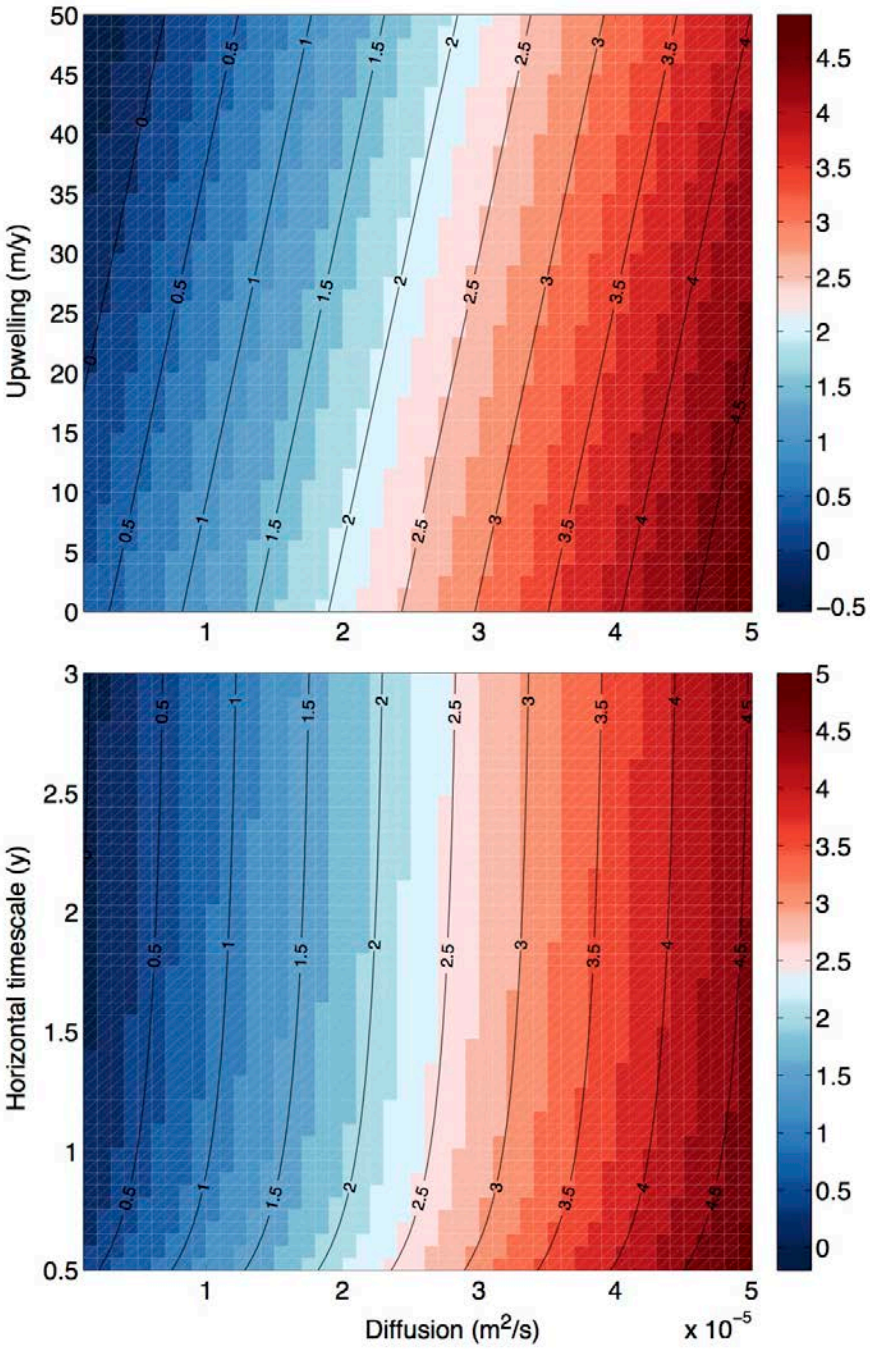

Fig. S2. Model sensitivity of Sta. 3 imbalance of sources and sinks to physical parameters.

The N_2O imbalance (nmol L^{-1} d^{-1}) at the peak N_2O concentration are shown for varying vertical diffusion and (top) upwelling velocities and (bottom) horizontal restoration time scales. Vertical diffusion is the overwhelmingly important term, and, for commonly observed diffusivity values, a net source > 1 nmol L^{-1} d^{-1} can be generated regardless of upwelling velocity or horizontal physics.

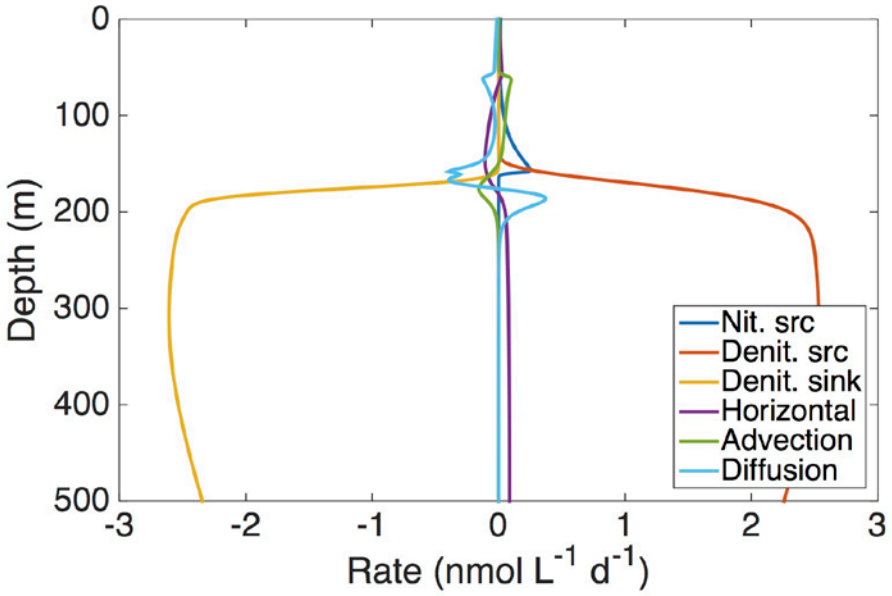

Fig. S3. 1–D profiles of modeled sources and sinks.

Average contributions to overall N_2O sources (src) and sinks via biology and physics for the model runs that include a parameterization of horizontal transport and vertical advection and diffusion.

Parameter	Description	Value	
w_{sink}	Particulate sinking velocity	1.2×10^{-4}	m s^{-1}
w_{up}	Upwelling velocity	8×10^{-7}	m s^{-1}
D_z	Turbulent diffusivity	4×10^{-5}	m^2 s^{-1}
$r_{P:C}^{rem}$	Redfield stoichiometry (*51*)	1/106	
$r_{P:C}^{den}$	Redfield stoichiometry (*51*)	1/106	
$r_{N:C}^{rem}$	Redfield stoichiometry (*51*)	16/106	
$r_{N:C}^{den}$	Anderson denit. stoichiometry (*52*, *53*)	104/106	
$r_{O_2:C}^{rem}$	Anderson stoichiometry (*52*)	150/106	
k_{rem}	Remineralization rate constant	9.3×10^{-7}	s^{-1}
K_{O_2}	Nitrification O_2 half saturation constant (*12*)	4	µmol L^{-1}
$K_{O_2}^{Nev}$	Nitrification O_2 threshold	2†	µmol L^{-1}
a_1	Nevison nitrification O_2 parameter (*21*)	0.26	µmol L^{-1}
b_1	Nevison nitrification parameter (*21*)	-0.0006	
k_{den}	Denitrification rate constant	1.9×10^{-7}	s^{-1}
$K_{NO_3^-}$	Denitrification NO_3^- half saturation constant	5	µmol L^{-1}
$k_{N_2O}^{Yam}$*	N_2O consumption constant (*19*)	6.0×10^{-9}	s^{-1}
$k_{N_2O}^{fast}$*	N_2O consumption to match observations	1.8×10^{-6}	s^{-1}
$K_{O_2}^{den}$	N_2O production O_2 poisoning (*26*)	1	µmol L^{-1}
$K_{O_2}^{sink}$	N_2O consumption O_2 poisoning (*26*)	0.3	µmol L^{-1}

Table S1. Parameters used in 1D model.

Models incorporated values as shown, with references where appropriate. †We used a lower nitrification cutoff than 4 µmol L^{-1} O_2 per Nevison et al. (*21*), to be more in line with observations by Martens-Habbena et al. (*12*). *Original model used a slower N_2O consumption rate parameterized as in Yamagishi et al. (*19*) as a net rate, but the new model required a faster consumption term to match observed rates.

Model	Baseline	With horizontal restoration	Varying BGC parameters only	No denitrification production
$[N_2O]_{max}$ (nM)	113 ± 34	96 ± 26	120 ± 34	74 ± 26
$z_{[N2O]max}$ (m)	133 ± 24	156 ± 35	135 ± 5	128 ± 23
SMS_{max} (nM/d)	0.62 ± 0.27	0.68 ± 0.29	0.65 ± 0.23	0.26 ± 0.13
z_{SMS} (m)	162 ± 31	168 ± 33	163 ± 6	158 ± 31
Δz offset (m)	29 ± 9	13 ± 17	29 ± 5	30 ± 9
$[O_2]$ @ $[N2O]_{max}$ (µM)	10.1 ± 2.7	3.4 ± 1.7	9.1 ± 2.6	14.6 ± 2.5
$[O_2]$ @ SMS_{max} (µM)	1.6 ± 0.6	1.4 ± 0.6	1.5 ± 0.7	2.5 ± 0.5

Table S2. N_2O profile characteristics under different modeling schemes.

Concentration and net sources minus sinks (SMS) peak characteristics for each of the Monte Carlo run types are shown. Brackets indicate concentrations of parameters, SMS the net N_2O production rate, z the depth, and Δz offset indicates how much deeper the SMS rate maximum is compared with the N_2O concentration maximum. The baseline model is the 1–D model used throughout the paper and described in the SOM. Model changes are included as headers, with BGC an abbreviation for biogeochemistry.

Sta.	Depth (m)	[N_2O] (nM)	[NO_2^-] (µM)	R* (nM/d)	P* (nM/d)	Net (nM/d)	Turnover (d)
1	25	86.1	0.64	2.6	9.3	6.8	11.9
	40	24.7	5.91	35.2	34.9	–0.4	0.9
	50	12.8	3.12	23.4	22.5	–0.8	0.7
	60	18.9	6.78	6.1	6.4	0.3	3.8
	100	19.4	7.46	4.2	4.3	0.1	5.8
	150	19.3	4.96	4.9	5.3	0.4	4.7
	250	15.7	2.66	3.5	3.5	0.0	5.7
	500	16.2	0.00	3.5	3.2	–0.2	6.0
2	85	96.2	0.14	1.0	5.5	4.4	27.2
	100	61.1	0.11	1.6	4.0	2.5	23.5
	115	30.0	0.88	2.1	2.1	0.0	19.9
	125	13.6	2.68	2.6	2.6	0.0	6.9
	140	56.0	3.89	2.7	6.8	4.1	10.2
	150	34.1	6.11	1.5	4.1	2.7	12.9
	250	6.8	3.03	1.4	1.4	0.0	18.5
	500	17.9	0.50	1.6	1.6	0.0	11.7
3	95	107.0	0.00	1.4	4.5	3.5	36.1
	100	86.4	0.00	1.6	1.6	0.0	64.6
	115	24.6	1.16	1.6	0.4	–1.6	18.1
	125	14.6	2.05	2.7	2.1	–0.5	8.5
	140	14.8	3.07	2.8	2.7	0.0	8.2
	150	14.2	3.91	2.8	1.4	0.0	14.8
	200	13.9	2.99	1.7	1.0	–0.4	15.1
	250	46.1	2.65	1.8	2.4	0.8	30.5

Table S3. Biogeochemical measurements in the ETNP

Concentration and reduction rate (R) measurements from the 3 stations in the ETNP. Calculated production rates (P) and the net (P – R) are included. The turnover time is calculated as the N_2O concentration divided by the reduction rate if net N_2O sink or by the production rate if net source.